



In Situ Stress State of the Ruhr Region (Germany) and Its Implications for Permeability Anisotropy

Michał Kruszewski^{1,2} · Giordano Montegrossi³ · Tobias Backers² · Erik H. Saenger^{1,2,4}

Received: 28 July 2020 / Accepted: 16 August 2021 / Published online: 28 September 2021
© The Author(s) 2021

Abstract

In this study, we carried out reactivation potential analysis of discontinuities revealed from four exploration boreholes penetrating heavily faulted and folded Upper Carboniferous rock strata of the Ruhr region. We performed this study based on the notion that slip is controlled by the ratio of shear to effective normal stresses acting on a pre-existing plane of weakness in the prevailing stress field configuration. The results of this analysis were supported by indicators of localized fluid flow, both on micro- and macro-scales, which confirm relationship between secondary permeability and in situ stress state in the Ruhr region. Findings from this study, in conjunction with results of destructive laboratory testing, indicate that the steep NW–SE- and NNE–SSW-striking planar discontinuities are likely to be either close to the critical state or critically stressed in the in situ stress configuration in the Ruhr region. These planar structures, as evidenced by indicators of localized permeability, are the main fluid pathways in the studied region. The NE–SW-striking discontinuities, on the other hand, are most likely to be closed and hydraulically inactive in the prevailing stress state. Based on results gained from this study, implications for utilization of deep geothermal energy in the region were discussed.

Keywords Reservoir geomechanics · Geothermal geomechanics · Crustal stresses · Geothermal energy · Deep geothermal systems · Ruhr region

1 Introduction

It is generally accepted that fractures and faults are the main fluid conduits in the Earth's crust (Hickman et al. 1995). The in situ stress tensor is one of the major controls on the reservoir permeability anisotropy, where fractures and faults (regardless of scale) with high shear to normal stress ratios

(i.e., ones having high reactivation potential) are considered as primary fluid pathways in both crystalline and sedimentary formations (Barton et al. 1995; Ito and Zoback 2000; Moeck et al. 2009; Zoback 2007). The presence of these, so-called, critically stressed planes makes the permeability of crust about four times larger than for a case of an intact rock subjected to appropriate confining pressures (Townend and Zoback 2000). An understanding of reactivation potential of fractures and faults is a critical issue in the development of man-made, and especially conduction-dominated, geothermal systems. First, the success of such a system relies on the number of intersected permeable fractures and/or faults oriented favorably to the in situ stress tensor (Zoback 2007). Second, if a fault cutting a reservoir has high effective normal stresses acting on its plane (i.e., sealing fault), it can isolate fluid flow and compartmentalize a reservoir. On the contrary, fault with high dilational stresses may induce fluid leakage during drilling operations. Third, knowledge about reactivation potential of fractures and faults is important in cases where rock matrix permeability is insufficiently low and stimulation treatments are necessary to enhance it. Fracture initiation, in case of hydrofracturing, or reactivation,

✉ Michał Kruszewski
michal.kruszewski@ieg.fraunhofer.de

¹ Fraunhofer Research Institution for Energy Infrastructures and Geothermal Systems IEG, Am Hochschulcampus 1 IEG, 44801 Bochum, Germany

² Institute of Geology, Mineralogy, and Geophysics, Ruhr-University Bochum, Universitätsstraße 150, 44801 Bochum, Germany

³ Institute of Geoscience and Earth Resources, National Research Council of Italy, Via G. La Pira 4, 50121 Florence, Italy

⁴ Department of Civil and Environmental Engineering, Bochum University of Applied Sciences, Am Hochschulcampus 1, 44801 Bochum, Germany

in case of hydro-shearing, may be needed to generate flow paths and enhance reservoir productivity. Significant pore pressure disturbances during fluid injections, not adjusted to the prevailing in situ stress tensor and rock frictional properties, may reduce the frictional strength of faults and induce their either aseismic or, if the stress conditions will be sufficiently altered over a large area, coseismic shear slip. As a result, before an establishment of any deep geothermal system and carrying out subsequent stimulation efforts, in situ stress tensor and its effect on the fracture and fault network shall be well understood.

The Ruhr region is located in the heart of the North-Rhine Westphalia state in western Germany. It is one of the largest metropolitan areas of Europe with more than 5 million inhabitants extending over 130 km from west to east and 35 km from south to north, covering an area of $\sim 4600 \text{ km}^2$ between the valleys of the Ruhr, Emscher, Lippe, and Rhine rivers. The Ruhr district heating network supplies $6500 \text{ GWh year}^{-1}$ with an installed thermal capacity of 2310 MWth (Bartelt et al. 2013). The wider metropolitan region of Rhine-Ruhr is one of the largest district heating networks in the world, fed primarily by fossil fuels, i.e., coal and natural gas (Klaus et al. 2010). To meet national and international climate protection targets, this network is to be converted into a CO_2 -free energy network in the forthcoming decades (Wegener et al. 2019). The Ruhr region is defined by the rich coal-bearing layers of the Upper Carboniferous period, belonging to the sub-Variscan Trough, with hard coal extraction starting in the thirteenth century. In 2018, after more than 700 years of extensive hard coal mining, the last mine was decommissioned in the region. The conversion of the district heating system in the Ruhr region could rely on the use of its vast geothermal potential. Favorable conditions for establishing deep geothermal reservoirs may exist in the fractured sandstones of the Carboniferous age (Hahne and Schmidt 1982) and karstified and/or dolomitized carbonate rocks of the Devonian age (Przybycin et al. 2017;

Balcewicz et al. 2021). Devonian carbonates were intersected at depths between ~ 4500 and $\sim 6000 \text{ m}$ in several deep exploration boreholes, north from the Ruhr region (Eder et al. 1983; Drozdowski 1993; Hesemann 1965), and are outcropping south of the Ruhr region in the vicinity of Wuppertal, Schwelm, Hagen, and Iserlohn (Balcewicz et al. 2021; Meschede and Warr 2019) (Fig. 1). Based on the temperature profiles from exploration boreholes in the northern part of the Ruhr region gathered in this study (Fig. 2), the deepest borehole in the region (i.e., Münsterland 1) (Hesemann 1965), and temperature measurements from local coal mines (Wedewardt 1995), the average geothermal gradient amounted to $\sim 36^\circ\text{C km}^{-1}$. As a consequence, for reservoir depths between ~ 4500 and $\sim 6000 \text{ m}$, temperatures of ~ 170 up to $\sim 230^\circ\text{C}$ can be expected (assuming temperature of 10°C at the surface). Such thermal conditions may enable not only heat but also electricity production (Hettiarachchi et al. 2007) if sufficient permeability exists in situ. Due to the well-developed industrial and private infrastructure in the Ruhr region, there is a great interest in utilizing geothermal energy sources, being it either mine energy storage (e.g., Hahn et al. 2017) or deep geothermal systems (e.g., Balcewicz et al. 2021), and simultaneously a strong necessity for understanding and monitoring possible movements on major discontinuities and related seismic risks.

The main aim of this study is to investigate the fracture behavior under present-day stress tensor of the Upper Carboniferous rock strata of the Ruhr region and assess its effect on fluid flow. To do this, we use the slip tendency analysis, where we resolve shear and dilational stresses along pre-existing planar features, localized with borehole logging methods, and evaluate their slip and dilation potentials. Results of this analysis were compared with indicators of localized fluid flow based on observations of fluid loss during drilling operations, high-quality temperature log, and macro-scale observations of fault leakage. We re-evaluated available in situ stress data, coming from the coal mining

Fig. 1 A simplified geological interpretation of the northern part of the DEKORP 2-N seismic line (DEKORP 1990) with major faults (marked in red) and the Münsterland 1 well (marked with a black triangle) intersecting the top of Devonian layers (after Drozdowski 1988)

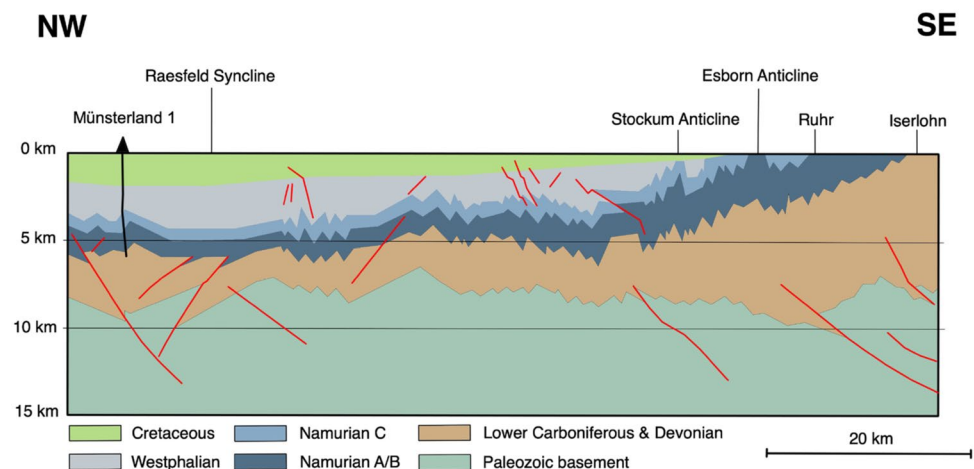
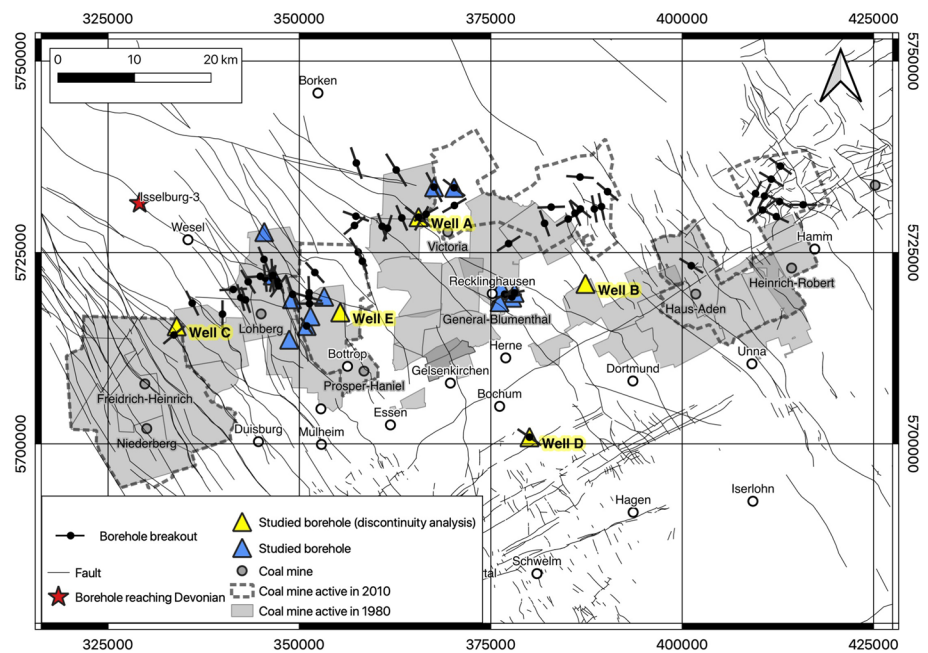


Fig. 2 The stress map of the Ruhr region with major fault systems (after NRW 2021), coal mines, boreholes investigated in this study, and borehole breakouts from Reinecker et al. (2008) (with increasing length of the line indicating higher quality of a stress indicator in accordance with Heidbach et al. (2018))



industry, across the Ruhr region and derived linearized pore pressure and in situ stress gradients. We used results from destructive laboratory testing and field measurements to constrain the frictional properties of fractured rocks within the Ruhr region. Using the slip tendency analysis, the potential for shear slip along pre-existing discontinuities, from four exploration boreholes, with respect to the in situ stress tensor was investigated and reactivation potential of the penetrated planar features assessed. Based on results gained from this study, implications for utilization of deep geothermal energy in the region were discussed.

2 Geological Setting

The coal-bearing strata of the Ruhr region belong to the external fold and thrust belt of the latest stage of the Variscan orogen, located east of the Wales–Brabant Massif (Brix et al. 1988). The Variscan orogenic belt was formed during the Late Paleozoic convergence of the Euramerican and Gondwanaland continental masses (Ziegler 1990). The collision and convergence took place during the Devonian and Carboniferous geologic periods.

The Ruhr region is influenced by two main fault systems. The major faults strike in the NE–SW direction with dips ranging from steeply inclined to bed-parallel reaching lengths of up to 40 km. These reverse type faults have horizontal displacements in the order of tens to hundreds of meters with few reaching horizontal displacements of ~ 2500 m. The reverse faults are dissected by multiple NW–SE oriented normal faults resulting in a horst-and-graben structure with few strike-slip faults of various

orientations also being observed in the region (Brix et al. 1988). Folds, mainly NE–SW oriented, vary significantly in shape and dimension with wavelengths of up to 10 km, increasing towards the north, having amplitudes in the order of several hundred meters.

Extensive hard coal mining activities exposed thick molasse-type clastic sediments of the Upper Carboniferous age ranging from shales, silt- to coarse-grained sandstones with 2–2.5 m thick coal seams of varied strength, all heavily deformed by thrusting and folding (Bachmann et al. 1971). North of the Ruhr region, thick, in places up to ~ 1800 m, Cretaceous strata overlays the Upper Carboniferous sequences (Drozdowski 1993). Four deep exploratory boreholes, located north of the Ruhr region i.e., Münsterland 1 (Hesemann 1965), Versold 1, Isselburg 3 (Drozdowski 1993), and Vingerhoets 93 (Eder et al. 1983) have all reached Devonian units. Carbonate layers of the Middle and Upper Devonian age, being part of the Devonian Reef Complex, are outcropping south of the Ruhr region close to the city of Iserlohn (Fig. 1). Based on the study by Balcewicz et al. (2021) from outcropping Devonian carbonate strata in Wuppertal, Hagen, and Honnetal, similar strike and dip of discontinuities to the ones from the Upper Carboniferous strata was observed, which could potentially indicate lack of significant in situ stress decoupling at depth.

As for today, there is, however, no direct proof (i.e., confirmation from exploratory drilling) of Devonian carbonates underlying the coal-bearing Carboniferous layers in the Ruhr region. Nonetheless, the interpretation of the DEKORP 2-N seismic line (DEKORP 1990) indicates strong reflections, corresponding to the high material contrasts, at approximately 5000 m depth (Fig. 1). These reflections, according

to Franke et al. (1990), Drozdowski (1988), and Drozdowski (1993), are thought to be Devonian platform carbonates encountered in deep boreholes north of the region.

Based on laboratory studies carried out on rock samples from the Ruhr region it can be concluded that low matrix permeability of $< 10^{-18} \text{ m}^2$ characterizes sandstones of the Upper Carboniferous age (Stöckhert 2015; Nehler et al. 2016; Brenne 2016; Alber and Meier 2020; Stöckhert et al. 2020; Duda and Renner 2013) and permeability of $< 10^{-15} \text{ m}^2$ characterizes Devonian limestones and dolostones (Balcewicz et al. 2021). Matrix porosity of both rock formations does not exceed, on average, 5–7 % (Thielemann et al. 2001; Jorand et al. 2015; Stöckhert et al. 2020) with local increases of permeability being connected to the weaker coal layers (Alber and Meier 2020) especially those induced by mining activities (Thielemann et al. 2001).

3 Past Geomechanical Studies

The in situ stress state of the Ruhr region was investigated in several geomechanical surveys, performed predominantly in its northern parts with hydrofracturing and overcoring methods. From the 1970s to the mid-1990s, in situ tests were carried out primarily to optimize the design of crosscuts and mine layouts or evaluate stress state in coal bed methane wells (Braunher 1976; Rummel et al. 1993; Müller 1989; Müller et al. 1991; Stelling and Rummel 1992). Most of the measurements were limited to depths of interest for the coal mining industry (i.e., $\sim 1500 \text{ m}$). Based on results from these surveys, magnitudes of minor, S_{hmin} , and major, S_{Hmax} , horizontal stress were acquired.

In the last 35 years, more than 1000 exploration boreholes were drilled in the northern part of the Ruhr region. In all of them, comprehensive logging programs were performed (Rudolph et al. 2010). This immense database allowed detailed analysis of borehole elongations and, as a result, estimation of S_{Hmax} orientation, θ_{SHmax} . A total length of 761 m of borehole breakouts from 3950 m of analyzed four-arm caliper logs in 40 boreholes spread across the Ruhr region were found by Müller (1989). The mean θ_{SHmax} from borehole breakout from his analysis amounted to $149 \pm 36^\circ$. Reinecker et al. (2008), carrying out a similar study, observed borehole breakouts in 51 boreholes in the Ruhr region with a total length of breakout intervals of 3014 m. The length-weighted θ_{SHmax} indicated by Reinecker et al. (2008) amounted to $168 \pm 48^\circ$, whereas the number-weighted θ_{SHmax} to $160 \pm 40^\circ$.

Based on information from above-mentioned studies, Ruhr region can be separated into two main stress units in terms of θ_{SHmax} with the boundary laying at the General Blumenthal mine (Fig. 2). The eastern part of the region is characterized by a transition from an NNW–SSE θ_{SHmax} in

its easternmost parts (i.e., mine Westfalen) to an NW–SE orientation in the westernmost parts (i.e., Haus Aden and Heinrich-Robert mines), which accordingly to Rummel et al. (1993) is due to the influence of regional faulting of the coal-bearing layers. The western part is characterized by θ_{SHmax} ranging from the N–S in its central part (i.e., Lohberg and General Blumenthal mines), and reorientation from NNW–SSE to NW–SE in its most western parts (i.e., Friedrich Heinrich and Niederberg mines), which accordingly to Rummel et al. (1993) is due to the influence of the graben structure of the Lower Rhine Bay.

4 Methodology

4.1 In Situ Stress State

The information about the magnitudes of the principal in situ stresses and pore pressure, P_p , in the Ruhr region, collected throughout this study, was based on re-evaluated data from Wedewardt (1995), Braunher (1976), Rummel et al. (1993), Müller (1989), Müller et al. (1991), Stelling and Rummel (1992), unpublished reports by Solexperts GmbH (Rummel and Weber 1994) as well as on results from drilling operations and geophysical logging from 17 wells in the Ruhr, and adjacent, regions within the Carboniferous layers acquired in this study (well locations presented in Fig. 2). The mentioned dataset included (i) 115 measurements of S_{hmin} from which depth was known for 80 measurements, (ii) 80 measurements of S_{Hmax} from which depth was known for 49 measurements, (iii) 17 measurements of vertical stress, S_v , based on geophysical logging, and (iv) pore pressure magnitudes acquired from 233 measurements of the density of water sampled from the local coal mines between 20 and 1470 m depth and fluid densities applied during drilling operations in the studied boreholes (Fig. 2).

4.2 Slip and Dilation Tendency Analysis

The fluid flow along any discontinuity depends primarily on the in situ stress tensor and its positioning in the subsurface (Barton et al. 1995). Once the in situ stress tensor is well understood, acting shear, τ , and effective normal, σ_n , stresses along any arbitrarily oriented planar feature can be resolved (Jaeger et al. 2007). Subsequently, in accordance with the Amonton's law, slip tendency, T_s , defined as a ratio between τ and σ_n , can be assessed (Morris et al. 1996)

$$T_s = \frac{\tau}{\sigma_n}. \quad (1)$$

Discontinuities with T_s approaching or exceeding frictional resistance for sliding, μ , are assumed to have increased likelihood for a shear movement

$$T_s \leq \mu. \quad (2)$$

The majority of discontinuity surfaces are not perfectly planar, but rather rough and undulating. In its undisturbed initial state, discontinuity surfaces mate to create the smallest possible apertures. However, once the in situ stress state is such that a discontinuity undergoes a degree of non-gouge forming microshear movement, asperities will slide over each other, resulting in discontinuity's self-propping effect and permeability increase (Esaki et al. 1999; Heffer and Lean 1993; Yeo et al. 1998). As a result, discontinuities with increased likelihood for a shear movement can be simultaneously assumed to be hydraulically active. On the other hand, discontinuities with low T_s are considered to have low fluid flow potential (Barton et al. 1995; Morris et al. 1996) and are expected to be "locked" in the in situ stress state.

Based on Gudmundsson (2000) and Gudmundsson et al. (2002) it is known, that extensional fractures also act as fluid-conducting features. To investigate the tendency of a discontinuity to dilate in an acting stress state, dilation tendency, T_d , being described as a potential for a given discontinuity to dilate under a given 3D in situ stress tensor was computed (Ferrill et al. 1999):

$$T_d = \frac{\sigma_1 - \sigma_n}{\sigma_1 - \sigma_3}, \quad (3)$$

where σ_1 and σ_3 are the maximum and minimum effective principal stresses, respectively.

To assess how close a given cohesionless discontinuity is to the critical state (i.e., failure), Coulomb's Failure Function, CFF , was computed (Zoback 2007):

$$CFF = \tau - \mu\sigma_n. \quad (4)$$

Negative CFF values describe stable planar feature, as acting τ are insufficient to overcome its resistance to sliding. In the case of CFF approaching or being equal to zero, frictional sliding on a pre-existing discontinuity is likely to occur.

4.3 Discontinuity Geometry

To evaluate the influence of the in situ stress tensor on the reservoir permeability, geometry of discontinuities (expressed by strike and dip angle) were acquired from dipmeter logs from three old deep vertical coal exploration boreholes. Although results from dipmeter logs are used primarily to indicate bedding planes, it is widely known that such logs provide information on faults, folds, discontinuities, nonconformities, and pre-existing fractures (Rider 1986). As slip tendency analysis is a method applicable for any planar structure or feature (Finkbeiner et al. 1997), we use it for all discontinuities registered with dipmeter logs. We do not distinguish between bedding planes, faults, or

fractures, but rather analyze the dataset as a whole in a statistical manner. In the fourth well, which is a recent shallow exploration well, we have used available results from an acoustic borehole imager tool, indicating pre-existing natural fractures. The four boreholes, penetrating the Upper Carboniferous strata of the Ruhr region, are located in four different sections of the studied region (Fig. 2), which allows for informed conclusions for the whole studied region. In addition to discontinuity geometry information, we use results from geophysical logging (i.e., borehole diameter, gamma ray, bulk density, and P-wave velocity logging) for preliminary lithology discrimination. The geophysical logging data was later smoothed for presentation. As no information from mud logging was available, we do not make an attempt to constrain detailed lithological profiles from the studied wells.

4.4 Permeability Indicators

For investigation of the relationship between localized fluid flow and registered planar features, verification data is necessary. Most often, such data include results from high-quality temperature logs, electrical images, Stoneley wave logs, flow-meter logs, or packer tests (Zoback 2007). In our case, only in one well high quality temperature log was accessible. This temperature log, available from a thermal response test, was used to determine the thermal properties of the formation rocks in situ. During the test, well was heated up for 84 hours and temperature was subsequently measured. To compute thermal anomalies, which are associated with fluid flow along a permeable discontinuities (Cornet 1989), we have calculated the temperature difference between the measured temperatures from the thermal response test and an average linearized temperature gradient computed from test results, following methodology presented in Ito and Zoback (2000). We make an assumption that any decrease of temperature during boreholes heating-up was related to an increase of permeability at the depth of a discontinuity.

In other three wells, due to the lack of any of the aforementioned verification data, we have used borehole observations based on fluid loss information registered during drilling operations. Fluid loss during drilling can be attributed to either (i) permeable matrix, (ii) large cavities, (iii) induced, or (iv) pre-existing discontinuities (Lavrov 2016). To initiate fluid losses, pre-existing discontinuities need to provide sufficient permeability for the drilling fluid to permeate. It means, that not every discontinuity will cause fluid loss, as they could be closed in the in situ stress state, filled with gouge, or mineralized. In the case of an open discontinuity, and especially for connected fracture networks, its capacity for accepting drilling fluid will increase and it will lead to loss of drilling fluid ranging from seepage to total losses. Drilling fluid loss data commonly contains a certain degree

of error, as it is recorded primarily by the drilling crew in real-time during drilling operations. The loss of fluid is most often registered by indicating depth of the fluid loss and measuring volume of fluid lost into the adjacent formation. In our case, the latter was not available and only depth of the fluid loss was known. To eliminate the uncertainty connected to the actual fluid loss depth along the well and by taking into account possible depth mismatch, a moving window of 2 m for each fluid loss depth point registered during drilling was applied. Subsequently discontinuities detected within ± 2 m of fluid loss depth were assumed to be responsible for the fluid flow at that depth.

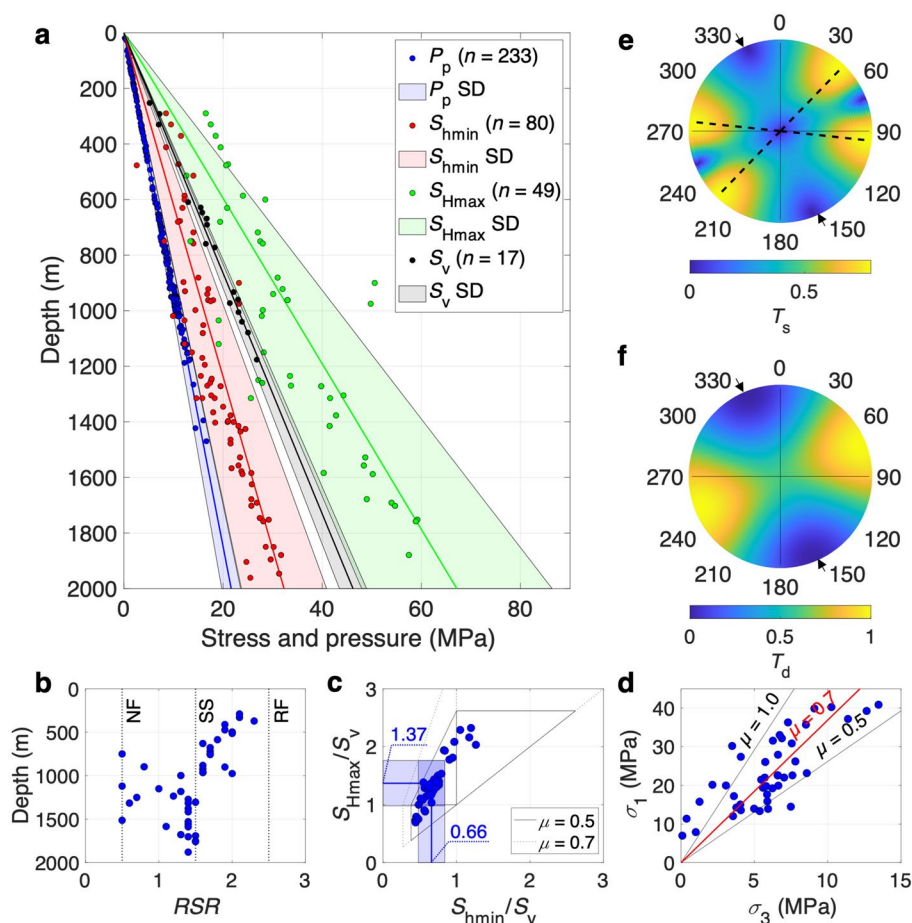
5 Results

5.1 In Situ Stress State

A compilation of in situ stress magnitude measurements across the Ruhr region is presented in Fig. 3a. Acquired data resulted in an average linearized P_p gradient of

$10.8 \pm 1.0 \text{ MPa km}^{-1}$. An average linearized S_v gradient amounted to $23.1 \pm 1.3 \text{ MPa km}^{-1}$. Acquired in situ stress data resulted in an average linearized S_{hmin} gradient of $16.1 \pm 4.3 \text{ MPa km}^{-1}$, whereas the average linearized S_{Hmax} gradient amounted to $33.6 \pm 9.6 \text{ MPa km}^{-1}$. The S_{hmin}/S_v ratio for the Ruhr region amounted to 0.66 ± 0.18 and the S_{Hmax}/S_v ratio to 1.37 ± 0.39 (Fig. 3c). Considerable scatter of both S_{hmin} and S_{Hmax} values between ~ 600 and ~ 1200 m depth was observed (Fig. 3a). It is expected that such scatter could be related to the influence of the coal mining on the in situ stress magnitudes. Based on Fig. 3b, it can be observed that transpression (Dewey et al. 1998) with regime stress ratio, RSR , computed after Simpson (1997), amounting to ~ 2 , was observed in the upper-most depths until approximately 600 m. Between depths of 600 and 1000 m, transition from transpression to a strike-slip regime was observed ($1.5 < RSR < 2$). Below that depth and until 2000 m, in situ stress measurements indicate predominantly strike-slip stress regime ($RSR \sim 1.5$). Both pure normal and reverse faulting regimes, can be considered as rather unlikely in the Ruhr region, as seen in Fig. 3b.

Fig. 3 **a** The present-day state of stress of the Ruhr region (shaded areas represent the uncertainty of pore pressure and principal in situ stress magnitudes; thick lines represent their average values; SD standard deviation); **b** regime stress ratio, RSR , from re-evaluated in situ stress measurements (NF normal faulting, SS strike-slip faulting, RF reverse faulting) computed according to Simpson (1997) ($n = 46$); **c** re-evaluated in situ measurements presented on a stress polygon plot with mean total stress ratios and their standard deviation ($n = 46$); **d** coefficient of sliding friction, μ , based on re-evaluated in situ measurements (line of best fit marked in red) computed according to Zoback and Townend (2001) ($n = 46$); **e** absolute slip, T_s , and **f** dilation, T_d , tendencies for the Ruhr region based on extrapolated linear stress and pore pressure gradients from this study and average θ_{SHmax} from Reinecker et al. (2008) with the direction of maximum T_s (arrows indicate θ_{SHmax})



5.2 Frictional Properties

Figure 3d presents a compilation of in situ stress measurement from the Ruhr region, similar to the one presented in Zoback and Townend (2001), with theoretical relationships for various frictional coefficients, based on frictional-failure theory, represented with solid lines. As shown in this figure, ratio between maximum, σ_1 , and minimum, σ_3 , effective stress corresponds to a crust in a frictional-failure equilibrium state (Jaeger et al. 2007), where majority of coefficients of friction are falling between 0.5 and 0.85. This implies that the studied area is either critically stressed or close to the critical state in accordance with Coulomb frictional-failure theory (Zoback and Healy 1984, 1992) and coefficient of friction between 0.5 and 0.85 the most accurately describes rocks of the Ruhr region. Only a few data points indicated μ being slightly higher than 1 and smaller than 0.5. The line of best fit for the acquired dataset amounts to μ of ~ 0.68 . The results presented in Fig. 3d agree with laboratory studies on the triaxially deformed Ruhr sandstone samples by Duda and Renner (2013), Duda et al. (2019), and Ahrens et al. (2018) shown in Fig. 4, where the friction coefficient of an intact and fractured Ruhr sandstone amounts to 0.73 and 0.67, respectively. Hunfeld et al. (2017), on the other hand, indicated μ of ~ 0.5 for Carboniferous shales from direct shear tests. Stoekhert et al. (2020), based also on direct shear test results, proved that μ of clean Ruhr sandstone sample with clay-filled gouge, can amount to value as low as 0.12. For the slip tendency analysis, we assume μ being in range between 0.5 and 0.7 in the Ruhr region.

5.3 Slip and Dilation Tendency Analysis

Figure 3e, f presents the lower hemisphere stereographic projection of absolute T_s and T_d values for the Ruhr region based on average linearized pore pressure and in situ stress gradients from this study and average θ_{SHmax} for the Ruhr

region from Reinecker et al. (2008). It can be observed that discontinuities most favorably oriented for failure in the in situ stress tensor, with a maximum T_s of 0.79, are vertically dipping with strike angle of N6° E and N134° W (i.e., around 30° from θ_{SHmax}). The NE–SW striking fractures have a low T_s and are, thus, much less likely to experience frictional sliding. The dilation tendency is the highest for fractures striking along θ_{SHmax} and lowest for the ones striking perpendicular to it. It can be, therefore, said that the NW–SE- and NNE–SSW-striking discontinuities will be the preferential fluid flow pathways in the Ruhr region. The NE–SW striking fractures, with much higher normal effective stresses and low T_d , will be likely closed in the present-day stress state configuration and hydraulically dead. We confirm these findings below.

5.4 Permeability Verification

Discontinuity datasets from the four studied boreholes (locations in Fig. 2), as shown in Figs. 5, 6, and 7 were presented with (i) plots of fracture strike with well depth, (ii) three-dimensional Mohr graphs and, (iii) lower hemisphere stereographic projections of CFF normalized by a vertical stress. In each well slightly different θ_{SHmax} , based on the nearby in situ stress measurement, was assumed.

5.4.1 Well A

The well A is located in the vicinity of the former Victoria mine, north of General Blumenthal and Lohberg mines. In this borehole, breakout analysis indicated θ_{SHmax} of N127°W. The orientations of discontinuities obtained from a dipmeter log revealed low dip angles ($< 20^\circ$) between depths of 660 and 980 m. Below that depth and until 1100 m moderate dip angles ($< 40^\circ$) were observed, whereas between 1100 and 1170 m, again low ($< 20^\circ$) dip angles were revealed. The strike direction until

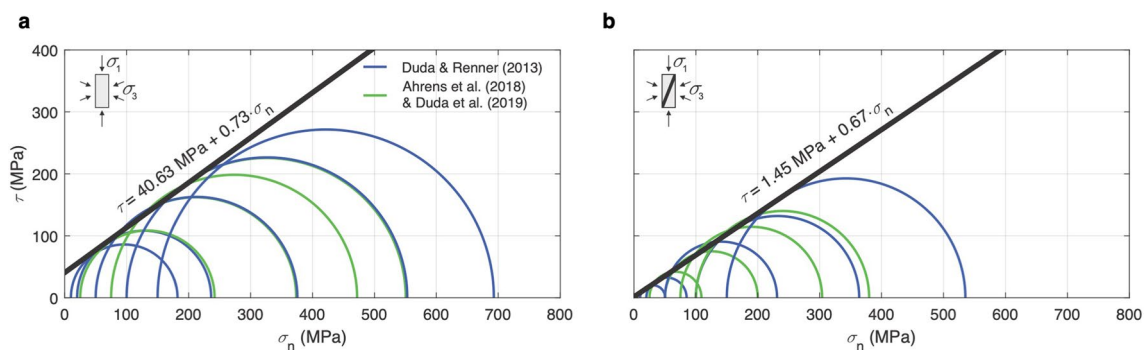


Fig. 4 Mohr's diagrams for **a** peak stress and **b** residual stress of triaxially deformed Ruhr sandstone samples at different confining pressures (Duda and Renner 2013; Duda et al. 2019; Ahrens et al. 2018).

The given equations describe linear envelopes (thick black lines) in the Mohr diagrams, that is, Mohr–Coulomb failure and friction criteria for **a** intact and **b** fractured rock, respectively

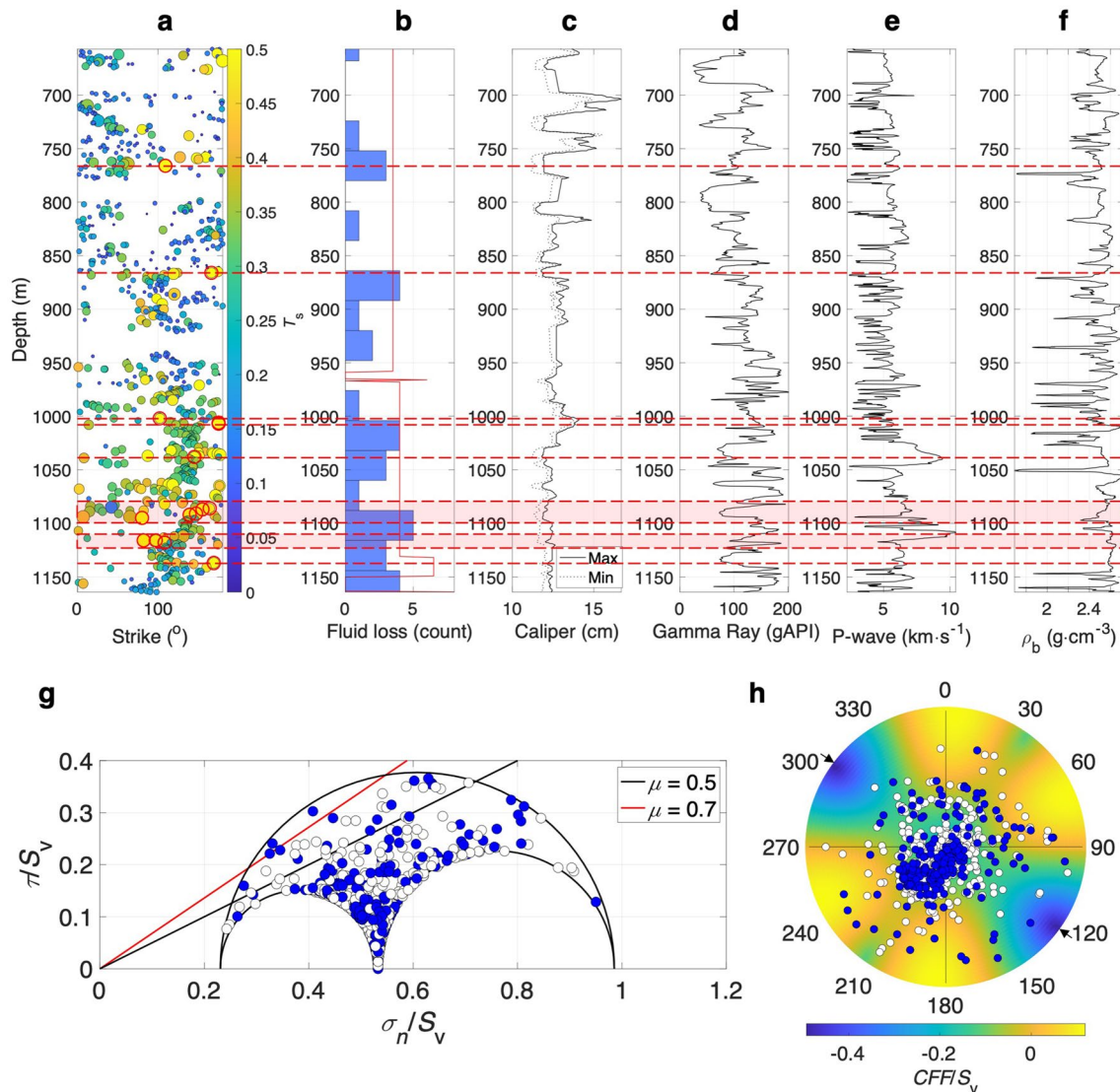


Fig. 5 Results of the slip tendency analysis in the well A: **a** strike of registered planar features with a color map indicating T_s (red outline and red dashed line indicate plane with $T_s \geq 0.5$ connected to a fluid loss; circle size represents increasing dip angle of a discontinuity. The actual dip angle value is presented in **h**; $n = 878$); **b** recorded fluid losses during drilling (red line presents percentage distribution of fluid losses from drilling report in tens of percent); **c** caliper log with

minimum and maximum registered borehole size; **d** gamma ray log; **e** P-wave velocity log; **f** bulk density log; **g** three-dimensional Mohr plot (blue circles indicate fluid loss; $n = 878$); **h** lower hemisphere stereographic projection of the CFF normalized by S_v with registered planar features (blue circles indicate fluid loss; $n = 878$) assuming μ of 0.5 (arrows indicate θ_{SHmax})

870 m depth does not have any major trend and is highly scattered. Below that depth and until the end of the log, discontinuities strike predominantly in the NW–SE direction. It was revealed that $\sim 4\%$ of the registered discontinuities have $T_s \geq 0.5$, from which $\sim 43\%$ experienced fluid loss. Planar features correlated with a fluid loss zone are observed at depths of 766 m (with strike of 109° and dip angle of 72°), 866 m ($166^\circ/51^\circ$), 1002 m ($102^\circ/50^\circ$), 1006 m ($175^\circ/71^\circ$), 1007 m ($175^\circ/71^\circ$), 1038 m ($145^\circ/55^\circ$), 1086 to 1092 m ($121^\circ/55^\circ$), 1095 m ($80^\circ/76^\circ$), 1116 to 1118 m (96°

$/67^\circ$), and 1137 m ($169^\circ/57^\circ$). Critically stressed planes correlate well with bulk densities of $\sim 2.5 \text{ g cm}^{-3}$, P-wave velocities of $\sim 5 \text{ km s}^{-1}$, and gamma ray values below 100 gAPI, indicating confinement within sandstone layers. The rest of fluid loss zones at depths of 825 m, between 875 and 950 m, and at 1150 m correlate with coal-bearing formations, which can be observed by a sharp bulk density decrease, low P-wave velocity, and a borehole diameter increase, all being indicative of penetration through weaker coal layers.

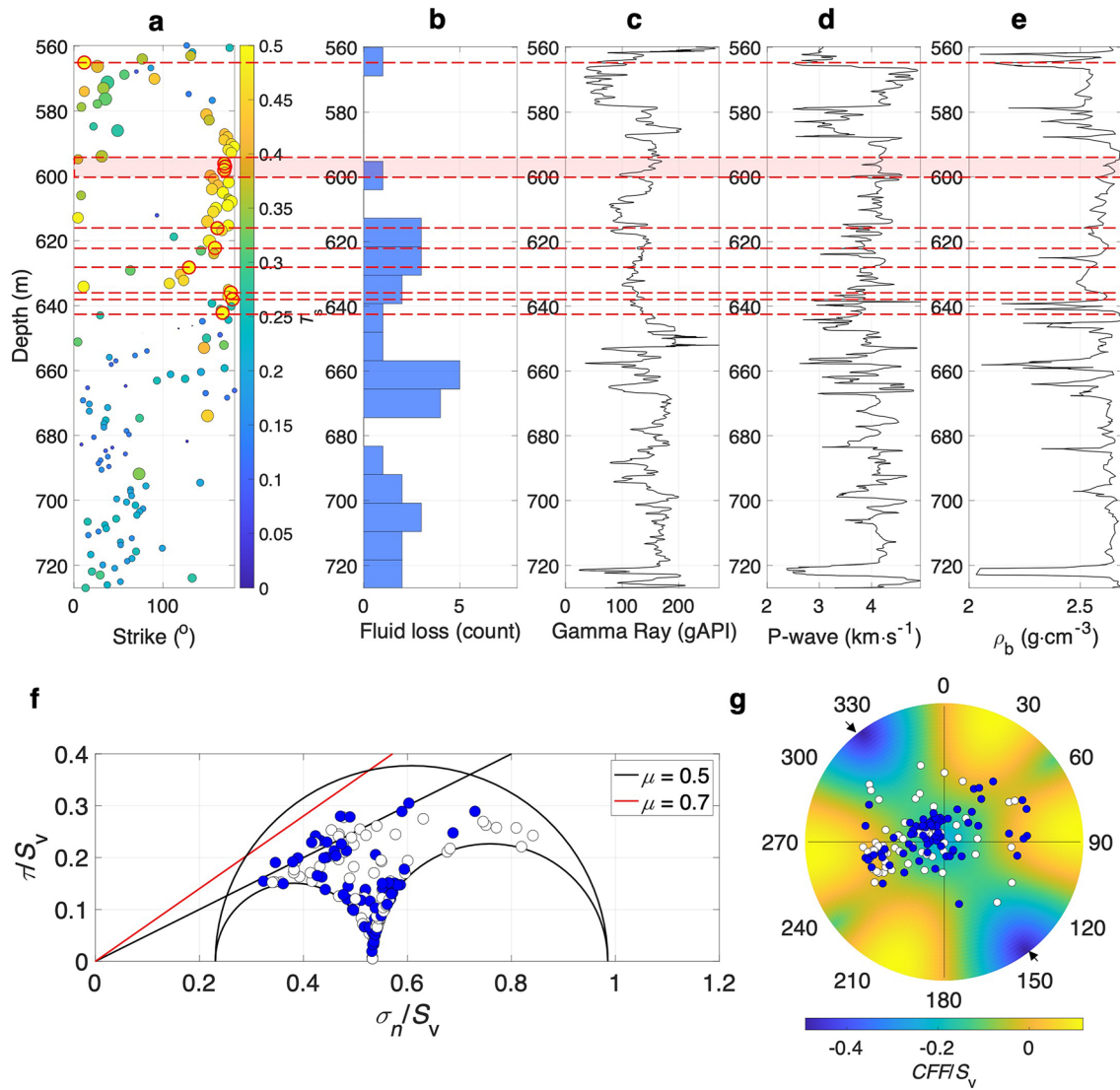


Fig. 6 Results of the slip tendency analysis in the well B: **a** strike of registered planar features with a color map indicating T_s (red outline and red dashed line indicate plane with $T_s \geq 0.5$ connected to a fluid loss; circle size represents increasing dip angle of a discontinuity. The actual dip angle value is presented in **g**); **b** recorded fluid losses during drilling; **c** gamma ray log; **d** P-wave velocity log; **e**

bulk density log; **f** three-dimensional Mohr plot (blue circles indicate fluid loss; $n = 155$); **g** lower hemisphere stereographic projection of the CFF normalized by S_v with registered planar features (blue circles indicate fluid loss; $n = 155$) assuming μ of 0.5 (arrows indicate θ_{SHmax})

5.4.2 Well B

The well B is located between the central and eastern part of the Ruhr region between former General Blumental and Haus Aden mines. For this borehole, θ_{SHmax} of N144°W was derived from hydrofracturing tests carried out in the former Haus Aden mine. Based on results from a dipmeter log from the well B, it was revealed that discontinuities between depth of 560 and 580 m have significantly varied dips ranging from 10 to 60°. Between depth of 580 and 640 m, high dip angles of approximately 50° were revealed. Below that depth and until 730 m, dip angles < 20° were observed.

The strikes between 560 and 580 m depth are significantly scattered without any major trend. Between 580 and 670 m discontinuities strike primarily in the NNW–SSE direction. Below that depth and until 730 m, registered planar features strike mainly in the NE–SW direction. In well B, ~ 10% of discontinuities have $T_s \geq 0.5$ from which 63 % experienced fluid loss. Discontinuities with $T_s \geq 0.5$ that experienced loss were observed at 565 m (12°/53°), between 596 and 598 m (169°/50°), 616 m (161°/51°), 622 m (158°/59°), 628 m (129°/51°), 635 m (176°/55°), 638 m (178°/53°), and at 642 m (167°/52°) depth. The fluid loss registered in the well B below 642 m, correlates well with the coal-bearing

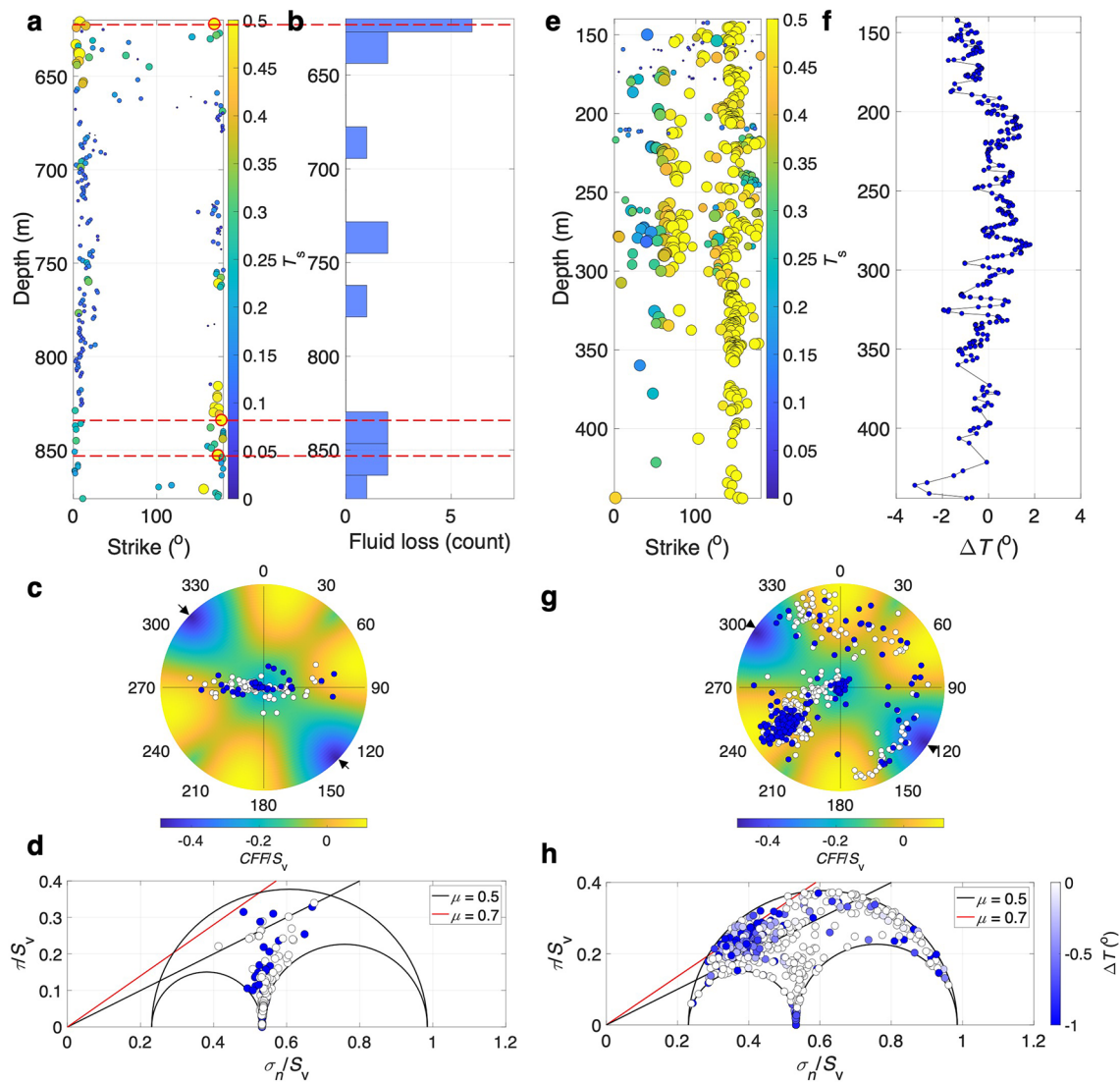


Fig. 7 Results of the slip tendency analysis in the well C (presented on the left side; $n = 230$) and well D (presented on the right side; $n = 525$): **a, e** strike of registered planar features with a color map indicating T_s (red outline and red dashed line indicate plane with $T_s \geq 0.5$ connected to a fluid loss; circle size represents increasing dip angle of a discontinuity. The actual dip angle values are presented

in **c** and **g**); **b** recorded fluid losses during drilling; **c, g** lower hemisphere stereographic projection of CFF normalized by S_v with registered planar features (blue circles indicate fluid loss) assuming μ of 0.5 (arrows indicate θ_{SHmax}); **d, h** three-dimensional Mohr plot (blue circles indicate fluid loss); **f** thermal anomaly registered while heating-up performed during thermal response test

layers (indicated by sharp bulk density and gamma ray decrease), which is especially visible at depths between 642 and 670 m, 680 m, and at 730 m. Based on a correlation of critically stressed discontinuities with bulk density log, all of the critically stressed planes are expected to be located within sandstone layers.

5.4.3 Well C

The well C is located in the most western part of the Ruhr region, close to the former Friedrich–Heinrich and Lohberg mines. The θ_{SHmax} amounting to N135°W was assumed for

the well C based on results from hydrofracturing tests carried out in the Friedrich–Heinrich mine. Based on the results from a dipmeter from this well, it was revealed that discontinuities located between depth of 620 and 650 m, have highly varied dip angles, proving no major trend. Below that depth and until 825 m, low dip angles ($< 10^\circ$) were registered. Between 825 and 875 m depth, dip angle increased to 20° . Registered discontinuities strike predominantly in the N-S direction. In the well C, only $\sim 3\%$ of registered discontinuities have $T_s \geq 0.5$. Three major fluid losses were localized in the analyzed interval i.e., between 625 and 650 m, 740 and 775 m, and between 830 and 875 m depth, with all

being correlated to the planes with high T_s values. Six planar features have $T_s \geq 0.5$ and fluid loss was observed in three of them. These three planar features, located at depth of 662 m (169°/64°), 834 m (178°/55°), and 852 m (174°/52°), correspond to the main fluid loss zones in the well. No geophysical logging was made available in this well to make a comparison with lithology.

5.4.4 Well D

The well D is located in the southern part of the Ruhr region within the city of Bochum. The θ_{SHmax} amounting to N124°W was assumed based on the drilling-induced fracture analysis performed in this well. Based on the acoustic borehole imager tool results, it was discovered that registered discontinuities have a highly varied dip angles ranging between 30 and 90° until approximately 300 m depth. Below that depth they become more consistent and amount to approximately 60°. The registered discontinuities strike predominantly in the NW–SE direction. A small group of discontinuities, striking perpendicularly to the NW–SE direction was registered between depth of 150 and 300 m. In the well D, ~ 50% of registered discontinuities have $T_s \geq 0.5$, from which ~ 61% have thermal anomaly of $\geq 0.5^\circ\text{C}$. Based on the analysis of the high-quality temperature log for indication of permeable discontinuities, it was discovered that fractures striking between N140° W and N160° W direction with high dip angles between 50 and 70° are the most likely to be permeable i.e., are related to the highest thermal anomalies.

6 Discussion

6.1 In Situ Stress State

There are significant limitations to the constrained in situ stress dataset and extrapolation of the constructed average linearized in situ stress gradients for the Ruhr region to depths greater than 2000 m. To remove uncertainties related to the state of stress below 2000 m depth, in situ measurements below that depth are advised. Moreover, due to the past and ongoing mine water pumping activates in the Ruhr region, water table levels in the subsurface have been significantly reduced. Currently average water table level in coal mines amounts to approximately 600 m (Brücker and Preuße 2020; Gombert et al. 2018), where in some cases water levels reduced to 1200 m were observed. Such significant differences in mine water table levels will cause pore pressure disturbances and, as a result, reactivation potentials change. As a consequence, the effect of P_p changes on the in situ stress tensor in the Ruhr region cannot be regarded as marginal and shall be investigated prior to the development

of a deep geothermal system. This is especially true for locations in the vicinity of the former coal mines and mine water pumping stations. It remains, also, not clear if or to what extent in situ stress magnitudes used to constrain the proposed stress model were affected by the coal mining activities.

The majority of θ_{SHmax} data in the Ruhr region is of low quality (i.e., D–E quality category of stress indicator) and, thus, less reliable, with only few measurements being of higher (i.e., A–C quality category of stress indicator) quality (Heidbach et al. 2018). Few measurements, from which the majority being of low quality, indicate NE–SW θ_{SHmax} , being more or less perpendicular to the regional θ_{SHmax} (Baumann 1981). The reason for these “unexpected” θ_{SHmax} re-orientations may be either due to (i) wrongly reported reading from the caliper tool, (ii) mistakenly picked or misinterpreted borehole breakouts (i.e., extended drilling-induced tensile fractures in weak layers, collapsed pre-existing open fractures or filter cake along caved zones picked instead of borehole breakouts) [Reiter and Heidbach (2014) references therein], or (iii) a near-isotropic horizontal stress state which would cause significant rotations of stress due to small local stress sources (Heidbach et al. 2007). The latter of which, based on the acquired stress data from the region, can be ruled out and with the first two explanations being considered as the most likely.

6.2 Fluid Flow and Discontinuity Analysis

The friction coefficient of the Ruhr region, as proven with in situ measurements and confirmed by laboratory studies, varies between ~ 0.5 for clay-rich rocks and ~ 0.7 for sandstones. Such high scatter indicates that pre-existing fractures and/or faults will be significantly more stressed in the clay-rich layers than in the sandstone layers. Based on the investigation performed in this study, the most hydraulically conductive are found to be the steeply dipping NNE–SSW and NW–SE striking discontinuities. The direction of these discontinuities, as confirmed with the permeability indicators on borehole scale, is also the preferential direction of the fluid flow in the Ruhr region. The majority of the critically stressed planes are confined within sandstone intervals.

Fluid flow and discontinuity analysis indicates that in all four analyzed wells there are (i) relatively few discontinuities that dominate the flow and (ii) relatively low number of planar features that are critically stressed. Nonetheless, the results of this analysis prove that the intersected critically stressed pre-existing planar features are hydraulically conductive and a match between critically stressed planes and permeability indicators can be considered as very good. This was indicated by fluid losses at depths corresponding to the critically stressed planes and is especially visible in the depth-related plots, where, intervals with planes having

higher T_s values represent intervals where fluid losses were registered. Although fluid loss data cannot be used to give accurate estimates on reservoir permeability, it is still useful in a qualitative sense for indicating fluid-conducting features. The increased resolution of the verification data, i.e., more sophisticated drilling fluid loss data, would additionally reduce the uncertainty during critically stressed plane evaluation. However, even without detailed information on individual pre-existing planar features and limitations of the verification data set, a correlation between the in situ stress state and preferential direction of fluid flow was found for the rock mass of the Ruhr region in wells A, B, and C. Especially good correlation is seen in the well D, where great majority of critically stressed planes are related to the high thermal anomalies, proving their increased permeability. In cases where a fluid loss was not related to a critically stressed planes, it may have been instead related to a permeable coal-bearing layers, induced hydraulic fracture, or extensive borehole deformations (i.e., wash-outs or wide breakouts) developed during drilling operations.

Results from this study agree with conclusions made by Rudolph et al. (2010) who, based on 3D numerical modeling efforts and results from geophysical logging from exploration boreholes across the Ruhr region, observed that in the vicinity of the NW–SE striking faults within Carboniferous sandstone formations increased permeability exists. The hypothesis of the NW–SE and NNE–SSW direction of permeability could be also confirmed by surface methane emissions study by Thielemann and Littke (1999), who concluded that the majority of the emitted gas at the surface, in the vicinity of the city of Bochum, is emitted alongside an NNW–SSE direction. Thielemann et al. (2001) observed that NW–SE striking Sachsen and Munster faults, located in the vicinity of the city of Hamm, were responsible for a few-meter-wide methane emission zones, along longitudinal fault axes, sourced at ~ 800 m depth. Such an observation confirms the interconnectivity of permeable faults from the coal layers up to the surface. Reinewardt et al. (2009) showed that during the penetration of the NW–SE striking Krudenburg fault, which dips around 80° to the west and has a thickness of ~ 80 m, within the Prosper-Haniel mine in 1982, major water and mud inflows in volumes between 0.3 and $18 \text{ m}^3 \text{ h}^{-1}$ were observed at all fault sections causing major disruptions during mining operations. Attempts of sealing the highly permeable fault with grout were made with $> 75,000 \text{ m}^3$ water removed from the fault using relief boreholes and 5500 m^3 of grout injected into the fault via injection boreholes. High permeability was also observed during drilling through the NW–SE striking Blumenthal fault close to city of Recklinghausen (Pilger 1960). Fault penetration during coal mining activities created there a water ingress of $12 \text{ m}^3 \text{ h}^{-1}$ and strong methane outgassing. The aforementioned studies, although being on a much

bigger scale, confirm the hypothesis of the preferential direction of permeability within the Ruhr region, as confirmed on a borehole scale and, thus, confirm the strong codependence of the present-day in situ stress tensor and fluid flow.

Other factors contributing to the discontinuity bulk permeability including discontinuity cohesion, filling material, aperture, roughness, or the degree of re-mineralization (Barton et al. 1995) were not investigated in this study. These factors may create exceptions to the overall correlation between in situ stress tensor, discontinuities, and permeability. Based on pre-existing fracture filling analysis carried out in the well E (location in Fig. 2), also penetrating Carboniferous strata, it was discovered that sulfides are the most common fracture filling materials, followed by carbonate materials, and clay minerals. Al Ismail and Zoback (2016) proved that in clay-rich reservoirs, no direct relation between clay content and magnitude of permeability exists, with high permeabilities existing for both clay- and calcite-rich rocks. They indicated that as clay content increases, higher permeability reduction at increasing effective stress, in comparison with calcite-rich samples, exists. The permeability of clay-rich rocks is, thus, much more sensitive to effective stress, which emphasizes the importance of forecasting geothermal fluid production based on stress-dependent permeability in clay-rich reservoirs. Only comprehensive data analysis including geophysical and temperature logging, wellbore imaging, in situ flow testing, and core studies would fully evaluate the importance of all aforementioned factors on the fluid flow across pre-existing discontinuities in the Ruhr region.

6.3 Implications for Geothermal Energy Utilization

Due to the scarce intrinsic matrix porosity and permeability of the formation rocks in the Ruhr region, it is expected that the future geothermal systems will rely primarily on either fracture network systems, faults, or carbonate rocks with a high degree of dolomitization or karstification. To take the most benefit of the hydraulically active discontinuities, during the development of a deep geothermal system, drilling a geothermal borehole in a potential reservoir layer in NE–SW or WNW–ESE direction will be the most advantageous in terms of reservoir secondary permeability. If drilling in this direction will be connected to the penetration of the major NW–SE- or NNE–SSW-striking normal fault, seismic activity can be considered as likely. This is especially expected in case of hydraulic stimulation efforts in any of these structures. Once penetration of the major NW–SE-striking fault will be necessary, fault segments with lower T_s should be targeted. It is expected, that the NE–SW reverse faults are hydraulically dead and could act as a seal within a reservoir. To establish the best hydraulic connection between a geothermal doublet, wells could be drilled in either NW–SE or NNE–SSW direction to one another. Due to the potentially

likely occurrence of critically stressed fractures and faults in the Ruhr region, it is advised to perform comprehensive 3D geomechanical modeling and implement real-time seismic monitoring using traffic light systems or seismogenic index models to minimize seismic risks related to the exploration of deep geothermal resources. In addition, more comprehensive laboratory studies on the frictional properties under reservoir-specific conditions are sought.

7 Conclusions

In this study, we investigated the relationship between the in situ stress state and reservoir permeability in a heavily faulted and folded Upper Carboniferous rock mass of the Ruhr region. Based on the collected in situ stress data, the stress state of the Ruhr region remains relatively homogeneous and can be described predominantly by a strike-slip regime with pure normal and reverse regimes being considered as unlikely. The P_p gradient of the region amounts to $10.8 \pm 1.0 \text{ MPa km}^{-1}$, S_v gradient to $23.1 \pm 1.3 \text{ MPa km}^{-1}$, S_{hmin} gradient to $16.1 \pm 4.3 \text{ MPa km}^{-1}$, and S_{Hmax} gradient, with the highest uncertainty, to $33.6 \pm 9.6 \text{ MPa km}^{-1}$. S_{hmin}/S_v amounts to 0.66 ± 0.18 and S_{Hmax}/S_v to 1.37 ± 0.39 . In situ stress measurements below 2000 m depth are advised to better constrain the in situ stress tensor at greater depths in the Ruhr region. The slip tendency analysis of planar features located in four exploration wells suggests that only a small percentage of discontinuities registered by the dipmeter are critically stressed (i.e., favorably oriented for failure within the current stress field), whereas around half of all discontinuities registered by borehole imager tool are considered critically stressed. To establish relationships between orientations of planar features and fluid flow, we used data on both micro- and macro-scales. These data presented evidence that formation permeability is enhanced at depth intervals with brittle lithologies and critically stressed pre-existing discontinuities that are favorably oriented for failure within the current stress field. It was revealed that the steeply dipping NW–SE and NNE–SSW oriented discontinuities penetrated by the analyzed wells play an important role in providing fluid migration pathways in the low-permeability rocks of the Ruhr region. The critically stressed discontinuities are found to be better hydraulic conduits than discontinuities unfavorably oriented for failure (i.e., structures striking in the NE–SW direction) in the prevailing in situ stress tensor, which are considered to be closed and hydraulically dead. As it is expected that future geothermal systems in the Ruhr region will rely primarily on secondary permeability, drilling new geothermal boreholes in the NE–SW or WNW–ESE within a potential target layer will be the most beneficial in terms of reservoir bulk permeability.

Acknowledgements The authors would like to thank the Geologischer Dienst Nordrhein-Westfalen and the RAG Aktiengesellschaft for data provision. We especially thank Dr. Benedikt Ahrens from the Fraunhofer Research Institution for Energy Infrastructures and Geothermal Systems IEG for proofreading and providing frictional properties of the Ruhr sandstone. Additional thanks go to Mohamed Ibrahim Moursy from the RWTH Aachen University for data digitalization, Dr. Claudia Finger from the Fraunhofer Research Institution for Energy Infrastructures and Geothermal Systems IEG and Dr. Francesco Parisio from the Freiberg University of Mining and Technology for proofreading. We would also like to thank Prof. Dr. Oliver Heidbach from the Deutsches GeoForschungsZentrum GFZ for constructive discussions about the in situ stress state of the Ruhr region. The authors would like to express their deep appreciation to Mr. Gerd Klee from Solexperts GmbH for sharing in situ stress data from the Ruhr Carboniferous.

Funding Open Access funding enabled and organized by Projekt DEAL. This work was carried out in the framework of the 3D-RuhrMarie (FHprofUnt2016) project, which received funding from the Federal Ministry of Education and Research and geomecon GmbH.

Declarations

Conflict of interest The authors reserve the right not to be responsible for the topicality, correctness, completeness, and quality of the information provided. Liability claims regarding damage caused by the use of any information provided will be rejected. Conclusions made in this study are solely opinions of the authors and do not express the views of the employer, university, or funding agency.

Open Access This article is licensed under a Creative Commons Attribution 4.0 International License, which permits use, sharing, adaptation, distribution and reproduction in any medium or format, as long as you give appropriate credit to the original author(s) and the source, provide a link to the Creative Commons licence, and indicate if changes were made. The images or other third party material in this article are included in the article's Creative Commons licence, unless indicated otherwise in a credit line to the material. If material is not included in the article's Creative Commons licence and your intended use is not permitted by statutory regulation or exceeds the permitted use, you will need to obtain permission directly from the copyright holder. To view a copy of this licence, visit <http://creativecommons.org/licenses/by/4.0/>.

References

- Ahrens B, Gilbert JP, Kroll K, Duda M (2018) Thermomechanical characterization of subsurface seasonal thermal energy storage in the Ruhr metropolitan area. In: Proceedings of the German GeothermalCongress, 27–29. November 2018, Haus der Technik in Essen
- Al Ismail MI, Zoback MD (2016) Effects of rock mineralogy and pore structure on stress-dependent permeability of shale samples. *Philos Trans R Soc A Math Phys Eng Sci* 374(2078):20150428
- Alber M, Meier T (2020) Multifrac – grundlagenuntersuchungen zum konzept des multi-riss-basierten aufschlusses geothermischer lagerstätten im norddeutschen becken. Project report no FZK 0324138A/B (in German)
- Bachmann M, Michelau P, Rabitz A (1971) Das rhein-ruhr-revier. stratigraphie. *Fortschr Geol Rheinld Westf* 19:19–33
- Balcewicz M, Ahrens B, Lippert K, Saenger EH (2021) Characterization of discontinuities in potential reservoir rocks for geothermal

- applications in the Rhine-Ruhr metropolitan area (Germany). *Solid Earth* 12(1):35–58
- Bartelt M, Beck J, Donner O, Marambio C, Michels A, Ritzau M, Schrader K (2013) Perspektiven der fernwärme im ruhrgebiet bis 2050, Abschlussbericht, BET Büro für Energiewirtschaft und technische Planung GmbH, Aachen, 2013
- Barton CA, Zoback MD, Moos D (1995) Fluid flow along potentially active faults in crystalline rock. *Geology* 23(8):683–686
- Baumann H (1981) Regional stress field and rifting in western Europe. *Tectonophysics* 73:105–111
- Braunher G (1976) Spannungsuntersuchungen bei gebirgsschlaggefahr durch messung absoluter gebirgsspannungen, essen, schlussbericht zum zuwendungsantrag, rag-kenn-nr. 191
- Brenne S (2016) Hydraulic fracturing and flow experiments on anisotropic and pre-fractured rocks. Ph.D. thesis, Ruhr-University Bochum, Bochum, Germany
- Brix M, Drozdowski G, Greiling R, Wolf R, Werde V (1988) The N Variscan margin of the Ruhr coal district (Western Germany): structural style of a buried thrust front? *Geol Rundsch* 77:115–126
- Brücker C, Preuße A (2020) The future of underground spatial planning and the resulting potential risks from the point of view of mining subsidence engineering. *Int J Min Sci Technol* 30(1):93–98 (**Special issue on ground control in mining in 2019**)
- Cornet F (1989) Survey by various logging techniques of natural fractures intersecting a borehole. In: Proceedings of the 3rd International Symposium on borehole geophysics for mining, geotechnical and groundwater applications 2:559–569
- DEKORP (1990) Results of deep-seismic reflection investigations in the Rhenish massif. *Tectonophysics* 173(1):507–515 (**Seismic probing of continents and their margins**)
- Dewey J, Holdsworth R, Strachan R (1998) Transpression and transtension zones. *Geol Soc Lond Sp Publ* 135(1):1–14
- Drozdowski G (1988) Die wurzel der osning-Überschiebung und der mechanismus herzynischer inversionsstörungen in mitteleuropa. *Geologische Rundschau* (1910. Print)
- Drozdowski G (1993) The Ruhr coal basin (Germany): structural evolution of an autochthonous foreland basin. *Int J Coal Geol* 23(1):231–250
- Duda M, Renner J (2013) The weakening effect of water on the brittle failure strength of sandstone. *Geophys J Int* 192(3):1091–1108
- Duda M, Benedikt A, Kristian K, Paul GJ (2019) Thermomechanical effects of seasonal thermal energy storage in former subsurface mining structures. In: EGU General Assembly Conference Abstracts, EGU General Assembly Conference Abstracts, p 13108 (April)
- Eder F, Engel W, Franke W, Sadler P (1983) Devonian and carboniferous limestone-turbidites of the Rheinisches Schiefergebirge and their tectonic significance. In: Martin H, Eder FW(eds) Intracontinental fold belts, Springer, pp 93–124
- Esaki T, Du S, Mitani Y, Ikusada K, Jing L (1999) Development of a shear-flow test apparatus and determination of coupled properties for a single rock joint. *Int J Rock Mech Min Sci* 36(5):641–650
- Ferrill D, Winterle J, Wittmeyer G, Sims D, Colton S, Armstrong A (1999) Stressed rock strains groundwater at yucca mountain, Nevada. *GSA Today Publ Geol Soc Am* 2(5):2–8
- Finkbeiner T, Barton CA, Zoback MD (1997) Relationships among in-situ stress, fractures and faults, and fluid flow: Monterey formation, Santa Maria Basin, California. *AAPG Bull* 81(12):1975–1999
- Franke W, Bortfeld R, Brix M, Drozdowski G, Dürbaum H, Giese P, Janoth W, Jödicke H, Reichert C, Scherp A et al (1990) Crustal structure of the Rhenish massif: results of deep seismic reflection lines dekorb 2-north and 2-north-q. *Geol Rundsch* 79(3):523–566
- Gombert P, Sracek O, Koukouzas N, Gzyl G, Valladares S, Frączek R, Klinger C, Areces AB, Chamberlain J, Paw K, Pierzchala L (2018) An overview of priority pollutants in selected coal mine discharges in Europe. *Mine Water Environ* 38:16–23
- Gudmundsson A (2000) Active faults and groundwater flow. *Geophys Res Lett* 27:2993–2996
- Gudmundsson A, Fjeldskaar I, Brenner SL (2002) Propagation pathways and fluid transport of hydrofractures in jointed and layered rocks in geothermal fields. *J Volcanol Geoth Res* 116(3):257–278
- Hahn F, Brüggemann N, Bracke R, Alber M (2017) Geomechanical characterization of the upper carboniferous under thermal stress for the evaluation of a high temperature—mine thermal energy storage (HT-MTES). In: EGU General Assembly Conference Abstracts. EGU General Assembly Conference Abstracts, p 14506 (April)
- Hahne C, Schmidt R (1982) Die Geologie des Niederrheinisch-WestfälischenSteinkohlengebietes: Essen, Verlag Glückauf, p. 106
- Heffer K, Lean J (1993) Earth stress orientation—a control on, and guide to, flooding directionality in a majority of reservoirs. In: Bill L (ed) Reservoir characterization III. PennWell Books, Tulsa, pp 799–822
- Heidbach O, Reinecker J, Tingay M, Müller B, Sperner B, Fuchs K, Wenzel F (2007) Plate boundary forces are not enough: second- and third-order stress patterns highlighted in the world stress map database. *Tectonics* 26(6). <https://doi.org/10.1029/2007TC002133>
- Heidbach O, Rajabi M, Cui X, Fuchs K, Müller B, Reinecker J, Reiter K, Tingay M, Wenzel F, Xie F, Ziegler M, Zoback ML, Zoback M (2018) The world stress map database release 2016: crustal stress pattern across scales. *Tectonophysics* 744:484–498
- Hesemann, J., 1965, Die Ergebnisse der Bohrung Münsterland 1: Forschungsberichte desLandes NordrheinWestfalen: Köln, Westdeutscher Verlag, v. 1468, p. 70
- Hettiarachchi HM, Golubovic M, Worek WM, Ikegami Y (2007) Optimum design criteria for an organic Rankine cycle using low-temperature geothermal heat sources. *Energy* 32(9):1698–1706
- Hickman S, Sibson R, Bruhn R (1995) Introduction to special section: mechanical involvement of fluids in faulting. *J Geophys Res Solid Earth* 100(B7):12831–12840
- Hunfeld L, Niemeijer A, Spiers C (2017) Frictional properties of simulated fault gouges from the seismogenic Groningen gas field under in situ p-t-chemical conditions. *J Geophys Res Solid Earth* 122(11):8969–8989
- Ito T, Zoback MD (2000) Fracture permeability and in situ stress to 7 km depth in the ktb scientific drillhole. *Geophys Res Lett* 27(7):1045–1048
- Jaeger J, Cook N, Zimmerman R (2007) *Fundamental of Rock Mechanics*, 4th Edition, Wiley-Blackwell, ISBN: 978-0-632-05759-7, 2007
- Jorand R, Clauser C, Marquart G, Pechnig R (2015) Statistically reliable petrophysical properties of potential reservoir rocks for geothermal energy use and their relation to lithostratigraphy and rock composition: the NE Rhenish massif and the lower Rhine embayment (Germany). *Geothermics* 53:413–428
- Klaus T, Vollmer C, Werner K, Lehmann H, Müschen K (2010) *Energieziel 2050: 100% strom aus erneuerbaren quellen*. Umweltbundesamt, Dessau
- Lavrov A (2016) Chapter 5—mechanisms and diagnostics of lost circulation. In: Lavrov A (ed) *Lost circulation*. Gulf Professional Publishing, Boston, pp 99–162
- Meschede M, Warr LN (2019) *The Geology of Germany – a Process-Oriented Approach*. –Series: Regional Geology Reviews. Springer, Heidelberg – Berlin, 304 pages ISBN 978-3-319-76102-2
- Moeck I, Schandelmeier H, Holl H-G (2009) The stress regime in a Rotliegend reservoir of the northeast German basin. *Int J Earth Sci* 98(7):1643–1654
- Morris A, Ferrill DA, Henderson DB (1996) Slip-tendency analysis and fault reactivation. *Geology* 24(3):275–278

- Müller W (1989) Messung der absoluten gebirgsspannungen im steinkohlenbergbau. *Glückauf-Forschungshefte* 50:105–112
- Müller W et al (1991) The stress state in the Ruhr coalfield. In: 7th ISRM Congress, International Society for Rock Mechanics and Rock Engineering, vol 3, pp. 1707–1711
- Nehler M, Andolfsson T, Stöckhert F, Renner J, Bracke R (2016) Monitoring fluid-rock interactions at in-situ conditions using computed tomography. In: *Proceedings, 41st Workshop on Geothermal Reservoir Engineering*, Stanford University, Stanford, California, 22–24th 2010, SGP-TR-209
- NRW G (2021) Datensatz großtektonik ruhrgebiet. Map, Geological Survey of North Rhine-Westphalia, Krefeld, Germany, <https://www.geoportal.nrw>. Accessed 1 June 2021
- Pilger A (1960) Über die Soleführung in den Störungen des Ruhrkarbons an einem Beispiel auf der Zeche Auguste Victoria. *Bergfreiheit* 9:287–293
- Przybycin AM, Scheck-Wenderoth M, Schneider M (2017) The origin of deep geothermal anomalies in the German molasse basin: results from 3d numerical models of coupled fluid flow and heat transport. *Geotherm Energy* 5(1):1–28
- Reinecker J, Tingay M, Müller B, Plenkens K, Thielmann M (2008) Analyse der bohrlochdaten von nordrhein-westfalen. Report (unpublished), Landesamt Krefeld, Krefeld, Germany
- Reinwardt K-J, Rosenstrater M, Enders G (2009) Auffahrung der 7. sohle des bergwerks prosper-haniel durch den krudenburg-sprung. *Glückauf (Essen)* 145(1):36
- Reiter K, Heidbach O (2014) 3-d geomechanical-numerical model of the contemporary crustal stress state in the Alberta basin (Canada). *Solid Earth* 5(2):1123–1149
- Rider MH (1986) *The geological interpretation of well logs*, 2nd edition, Gulf Pub., 1996
- Rudolph T, Melchers C, Minke A, Coldewey WG (2010) Gas seepages in Germany: revisited subsurface permeabilities in the German mining district. *AAPG Bull* 94(6):847–867
- Rummel F, Weber U (1994) Compilation of existing hydrofrac in-situ stress data for the Ruhr carboniferous. Report (unpublished), GEO-Mess-Systeme MESY GmbH, Bochum
- Rummel F, Weber U, et al (1993) Stress field in the coal mines of the Ruhr coal district. In: *The 34th US Symposium on Rock Mechanics (USRMS)*, American Rock Mechanics Association, Vol 34, pp. 609–612
- Simpson RW (1997) Quantifying Anderson's fault types. *J Geophys Res Solid Earth* 102(B8):17909–17919
- Stelling W, Rummel F (1992) Messung von primärspannungen durch hydraulik-fracturing auf dem bergwerk haus aden. *Das Markschheidewesen* 99(1):176–184
- Stöckhert F (2015) *Fracture mechanics applied to hydraulic fracturing in laboratory experiments*. Ph.D. thesis, Ruhr-Universität Bochum, Bochum, Germany
- Stoekchert F, Solibida C, Alber M, et al (2020) Hydraulic fractures in discontinuous, anisotropic and heterogeneous rock-a lab study. In: *ISRM International Symposium-EUROCK 2020*, International Society for Rock Mechanics and Rock Engineering
- Thielemann T, Littke R (1999) Examples of the methane exchange between litho-and atmosphere: the coal bearing Ruhr basin, Germany. In: Mastalerz M, Glikson M, Golding SD (eds) *Coalbed methane: scientific, environmental and economic evaluation*. Kluwer Academic Publishers, Dordrecht/Boston/London, pp 555–558
- Thielemann T, Krooss BM, Littke R, Welte DH (2001) Does coal mining induce methane emissions through the lithosphere/atmosphere boundary in the Ruhr basin, Germany? *J Geochem Explor* 74(1–3):219–231
- Townend J, Zoback MD (2000) How faulting keeps the crust strong. *Geology* 28(5):399–402
- Wedewardt M (1995) *Hydrochemie und Genese der Tiefenwässer im Ruhr-Revier*, vol 39. DMT, North Salt Lake, Bochum, Germany
- Wegener M, Schwarze B, Spiekermann K, Brosch K, Huber F, Müller M, Reutter O (2019) Modelling the great transformation in the Ruhr area. *Transport Res Proc* 41:231–239
- Yeo I, De Freitas M, Zimmerman R (1998) Effect of shear displacement on the aperture and permeability of a rock fracture. *Int J Rock Mech Min Sci* 35(8):1051–1070
- Ziegler PA (1990) *Geological atlas of western and central Europe*. Geological Society of London, Shell Internationale Petroleum Maatschappij, B.V., The Hague
- Zoback MD (2007) *Reservoir geomechanics*. Cambridge University Press, Cambridge
- Zoback M, Healy J (1984) Friction, faulting and «in situ» stress. *Ann Geophys* (1983) 2:689–698
- Zoback MD, Healy JH (1992) In situ stress measurements to 3.5 km depth in the Cajon pass scientific research borehole: Implications for the mechanics of crustal faulting. *J Geophys Res Solid Earth* 97(B4):5039–5057
- Zoback MD, Townend J (2001) Implications of hydrostatic pore pressures and high crustal strength for the deformation of intraplate lithosphere. *Tectonophysics* 336(1–4):19–30

Publisher's Note Springer Nature remains neutral with regard to jurisdictional claims in published maps and institutional affiliations.